Frequency map analysis and quasiperiodic decompositions.

Jacques Laskar
Astronomie et Systèmes Dynamiques,
CNRS UMR8028, IMCCE-Observatoire de Paris,
77 Av. Denfert-Rochereau, 75014 Paris, France

13 march 2003, revised 26 june 2003
proceedings of Porquerolles School, sept. 2001

1 Introduction

Frequency Map Analysis is a numerical method based on refined Fourier techniques which provides a clear representation of the global dynamics of many multi-dimensional systems, and which is particularly adapted for systems of 3-degrees of freedom and more. This method relies heavily on the possibility of making accurate quasiperiodic approximations of of quasiperiodic signal given in a numerical way. In the present paper, we will describe the basis of the frequency analysis method, focussing on the quasi periodic approximation techniques. Application of these methods for the study of the global dynamics and chaotic diffusion of Hamiltonian systems and symplectic maps in different domains can be found in (Laskar, 1988, 1990, Laskar and Robutel, 1993, Robutel and Laskar, 2001, Robutel, 2003, this volume, and Nesvorný and Ferraz-Mello, 1997) for solar system dynamics, and in (Papaphilippou and Laskar, 1996, 1998, Laskar, 2000, Wachlin and Ferraz-Mello,1998, Valluri and Merritt, 1998, Merritt and Valluri, 1999) for galactic dynamics. The method has been particularly successful for its application in particle accelerators (Dumas and Laskar, 1993, Laskar and Robin, 1996, Robin *et al.*, 2000, Comunian *et al.*, 2001, Papaphilippou and Zimmermann, 2002, Steier *et al.*, 2002), and was also used for the understanding of atomic physics (Milczewski *et al.*, 1997), or more general dynamical system issues (Laskar *et al.*, 1992, Laskar, 1993, 1999, Chandre *et al.*, 2001).

2 Frequency Maps

According to the KAM theorem (see Arnold *et al.*, 1988), in the phase space of a sufficiently close to integrable conservative system, many invariant tori will persist. Trajectories starting on one of these tori remain on it thereafter, executing quasiperiodic motion with a fixed frequency vector depending only on the torus. The family of tori is parameterized over a Cantor set of frequency vectors, while in the gaps of the Cantor set chaotic behavior can occur. The frequency analysis algorithm will numerically compute over a finite time span a frequency vector for any initial condition. On the KAM tori, this frequency vector will be a very accurate approximation of the actual frequencies, while in the chaotic regions, the algorithm will still provide some determination of the frequency vector, but in this region, complementary of the KAM tori, the frequency vector will not be uniquely defined.

Let us consider a n–DOF Hamiltonian system close to integrable in the form $H(I,\theta) = H_0(I) + \varepsilon H_1(I,\theta)$, where H is real analytic for $(I,\theta) \in B^n \times \mathbb{T}^n$, B^n is a domain of $\mathbb{R}^n$ and $\mathbb{T}^n$ is the n-dimensional torus. For $\varepsilon = 0$, the Hamiltonian reduces to $H_0(I)$ and is integrable. The equations of motion are then for all $j = 1, \dots, n$

$$\dot{I}_j = 0 \ , \quad \dot{\theta}_j = \frac{\partial H_0(I)}{\partial I_j} = \nu_j(I) \ ; \tag{1}$$

which gives $z_j(t) = z_{j0} e^{i\nu_j t}$ in the complex variables $z_j = I_j \exp i\theta_j$, where $z_{j0} = z_j(0)$. The motion in phase space takes place on tori, products of true circles with radii $I_j = |z_j(0)|$, which are described at constant velocity $\nu_j(I)$. If the system is nondegenerate, that is if

$$det\left(\frac{\partial \nu(I)}{\partial I}\right) = det\left(\frac{\partial^2 H_0(I)}{\partial I^2}\right) \neq 0 \tag{2}$$

the frequency map $F : B^n \longrightarrow \mathbb{R}^n; \quad (I) \longrightarrow (\nu)$ is a diffeomorphism on its image Ω, and the tori are as well described by the action variables $(I) \in B^n$ or in an equivalent manner by the frequency vector $(\nu) \in \Omega$. For a nondegenerate system, KAM theorem still asserts that for sufficiently small values of ε , there exists a Cantor set Ω_ε of values of (ν), satisfying a Diophantine condition of the form

$$|(k,\nu)| > \kappa_\varepsilon / |k|^m \tag{3}$$

for which the perturbed system still possesses smooth invariant tori with linear flow (the KAM tori). Moreover, according to Pöschel (1982), there exists a diffeomorphism

$$\Psi : \mathbb{T}^n \times \Omega \longrightarrow \mathbb{T}^n \times B^n; \qquad (\varphi,\nu) \longrightarrow (\theta, I) \tag{4}$$

which is analytical with respect to φ, C^∞ in ν, and on $\mathbb{T}^n \times \Omega_\varepsilon$ transforms the Hamiltonian equations into the trivial system

$$\dot{\nu}_j = 0 \ , \quad \dot{\varphi}_j = \nu_j \ . \tag{5}$$

For frequency vectors (ν) in Ω_ε, the solution lies on a torus and is given in complex form by its Fourier series

$$z_j(t) = z_{j0} e^{i\nu_j t} + \sum_m a_m(\nu) e^{i<m,\nu>t} \tag{6}$$

where the coefficients $a_m(\nu)$ depend smoothly on the frequencies (ν). If we fix $\theta \in \mathbb{T}^n$ to some value $\theta = \theta_0$, we obtain a frequency map on B^n defined as

$$F_{\theta_0} : B^n \longrightarrow \Omega \ ; \qquad I \longrightarrow p_2(\Psi^{-1}(\theta_0, I)) \tag{7}$$

where p_2 is the projection on Ω $(p_2(\phi,\nu) = \nu)$. For sufficiently small ε, the torsion condition (2) ensures that the frequency map F_{θ_0} is a smooth diffeomorphism.

2.1 Isoenergetic nondegeneracy

If the isoenergetic nondegeneracy condition of Arnold (1989) is verified

$$det \begin{pmatrix} \dfrac{\partial \nu(I)}{\partial I} & \nu(I) \\ \nu(I)^{\tau} & 0 \end{pmatrix} = det \begin{pmatrix} \dfrac{\partial^2 H_0(I)}{\partial I^2} & \dfrac{\partial H_0(I)}{\partial I} \\ \dfrac{\partial H_0(I)}{\partial I}^{\tau} & 0 \end{pmatrix} \neq 0 \tag{8}$$

then, if $\nu_n = \dfrac{\partial H_0(I)}{\partial I_n} \neq 0$, and for small enough ε, the application

$$(I_1, \dots, I_{n-1}, I_n) \longrightarrow \left(\frac{\nu_1}{\nu_n}, \dots, \frac{\nu_{n-1}}{\nu_n}, H \right) \tag{9}$$

is a diffeomorphism, and so will be its restriction F'_{θ_0} on $H^{-1}(h)$

$$(I_1, \dots, I_{n-1}) \longrightarrow \left(\frac{\nu_1}{\nu_n}, \dots, \frac{\nu_{n-1}}{\nu_n} \right) \tag{10}$$

When the isoenergetic nondegeneracy condition is verified, we can thus restrict ourself to an energy level $H = h$, and the frequency map $F_{\theta_0} : \mathbb{R}^n \to \mathbb{R}^n$ can be reduced to a map $F'_{\theta_0} : \mathbb{R}^{n-1} \to \mathbb{R}^{n-1}$.

3 Quasiperiodic approximations

The frequency analysis method and algorithms rely heavily on the observation that when a quasiperiodic function $f(t)$ in the complex domain $\mathbb{C}$ is given numerically, it is possible to recover a quasiperiodic approximation of $f(t)$ in a very precise way over a finite time span $[-T, T]$, several orders of magnitude more precisely than by simple Fourier analysis. Indeed, let

$$f(t) = e^{i\nu_1 t} + \sum_{k \in \mathbb{Z}^n - (1,0,\dots,0)} a_k e^{i\langle k,\nu \rangle t} \quad , \quad a_k \in \mathbb{C} \tag{11}$$

be a KAM quasiperiodic solution of an Hamiltonian system in $B^n \times \mathbb{T}^n$, where the frequency vector (ν) satisfies a Diophantine condition (3). The frequency analysis algorithm NAFF will provide an approximation $f'(t) = \sum_{k=1}^{N} a'_k e^{i\omega'_k t}$ of $f(t)$ from its numerical knowledge over a finite time span $[-T, T]$. The frequencies ω'_k and complex amplitudes a'_k are computed through an iterative scheme. In order to determine the first frequency ω'_1, one searches for the maximum amplitude of $\phi(\sigma) = \langle f(t), e^{i\sigma t} \rangle$ where the scalar product $\langle f(t), g(t) \rangle$ is defined by

$$\langle f(t), g(t) \rangle = \frac{1}{2T} \int_{-T}^{T} f(t) \bar{g}(t) \chi(t) dt \ , \tag{12}$$

and where $\chi(t)$ is a weight function (see next section). Once the first periodic term $e^{i\omega'_1 t}$ is found, its complex amplitude a'_1 is obtained by orthogonal projection, and the process is restarted on the remaining part of the function $f_1(t) = f(t) - a'_1 e^{i\omega'_1 t}$.

In the next sections, we provide the rigorous foundations of the frequency analysis algorithm by showing that this algorithm converges towards the frequency map described formally in the previous sections. It is interesting to see that the convergence of the frequency map algorithm will require some conditions on the frequency vector that will always be satisfied in the case of a KAM regular solution.

4 Convergence of Frequency Map Analysis.

Definiton. 1 *A weight function is a positive, even C^∞ function χ on $[-1,1]$ such that $\frac{1}{2}\int_{-1}^{1}\chi(t)dt = 1$. We will call the transform of χ, the C^∞ function on $\mathbb{R}$, φ_χ, defined as*

$$\varphi_\chi(x) = \langle e^{ixt}, 1\rangle_1^\chi \qquad \textit{where} \qquad \langle f(t), g(t)\rangle_T^\chi = \frac{1}{2T}\int_{-T}^{T} f(t)\bar{g}(t)\chi(t/T)\,dt \tag{13}$$

Lemma. 1 *If χ is a weight function, we have $\varphi_\chi(0) = 1$; $\varphi'_\chi(0) = 0$; $\varphi''_\chi(0) < 0$. For all $n \in \mathbb{N}$, we have $|\varphi_\chi^{(n)}(x)| < 1$, and there exists $M_n > 0$ such that $|x\varphi^{(n)}(x)| \leq M_n$ on $\mathbb{R}$.*

Proof. As $\chi(t)$ is even, $\varphi_\chi(x)$ is a real and even function, which implies $\varphi'_\chi(0) = 0$. We have $\varphi''_\chi(0) < 0$ as it is the integral of a strictly negative function. We have also $|\varphi^{(n)}(x)| \leq \frac{1}{2}\int_{-1}^{1}|t|^n\,\chi(t)dt < \frac{1}{2}\int_{-1}^{1}\chi(t)dt = 1$. On the other hand, using integration by parts, we obtain $|x\varphi^{(n)}(x)| \leq (\chi(1)+\chi(-1))/2 + \frac{1}{2}\int_{-1}^{1}\chi'(t)dt + n$.

Definiton. 2 *Let $\nu = (\nu_1, \nu_2, \ldots, \nu_n)$, and*

$$f(t) = e^{i\nu_1 t} + \sum_{k\in\mathbb{Z}^n-(1,0,\ldots,0)} a_k e^{i\langle k,\nu\rangle t}; \quad a_k \in \mathbb{C} \tag{14}$$

a quasi periodic function on $\mathbb{R}$. In the frequency map analysis, the approximation ν_1^T of ν_1 is obtained as the value of σ for which $\varphi(\sigma) = \left|\langle f(t), e^{i\sigma t}\rangle_T^\chi\right|$ is maximum in a neighborhood of ν_1.

Theorem. 1 *Let χ be a weight function, and $\varphi = \varphi_\chi$ its transform with the asymptotic expressions when $x \to \infty$*

$$\varphi(x) = \frac{g_0(x)}{x^n} + o\left(\frac{1}{x^n}\right), \quad \varphi'(x) = \frac{g_1(x)}{x^n} + o\left(\frac{1}{x^n}\right), \quad \varphi''(x) = \frac{g_2(x)}{x^n} + o\left(\frac{1}{x^n}\right), \tag{15}$$

where $n \geq 1$ and where $g_0(x), g_1(x)$ and $g_2(x)$ are bounded on $\mathbb{R}$. Let $f(t)$ be a quasi periodic function on the form (14), and for all k, $\Omega_k = \langle k,\nu\rangle - \nu_1$; and assume that $\sum_k |\frac{a_k}{\Omega_k^p}|$ is convergent for $p = 0, 1$, and n. Then for $T \to +\infty$, $\nu_1^T \to \nu_1$ and

$$\nu_1 - \nu_1^T = \frac{-1}{\varphi''(0)T^{n+1}}\sum_k \frac{\Re(a_k)}{\Omega_k^n} g_1(\Omega_k T) + o\left(\frac{1}{T^{n+1}}\right) \tag{16}$$

Proof. With $x = (\nu_1 - \sigma)T$, ν_1^T will be obtained for the maximum value of the modulus of

$$\psi(x) = \varphi(x) + \sum_{k \in \mathbb{Z}^n - (1,0,\ldots,0)} a_k \varphi\left(x + \Omega_k T\right) \tag{17}$$

or in an equivalent way, the maximum of its square $\psi(x)\bar{\psi}(x)$. This maximum thus fulfills the condition $\psi'(x)\bar{\psi}(x) + \psi(x)\bar{\psi}'(x) = 0$, that is

$$\begin{aligned} F(x,T) = \varphi(x)\varphi'(x) &+ \sum_{k,l} \Re(a_k \bar{a}_l)\ \varphi(x + \Omega_k T)\varphi'(x + \Omega_l T) \\ &+ \sum_k \Re(a_k)\left(\varphi(x)\varphi'(x + \Omega_k T) + \varphi'(x)\varphi(x + \Omega_k T)\right) = 0\ . \end{aligned} \tag{18}$$

Lemma. 2 *Let χ be a weight function, and $\varphi = \varphi_\chi$ its transform. Let us also assume that the series $\sum_k |a_k|$ and $\sum_k \left|\frac{a_k}{\Omega_k}\right|$ are convergent with sum S_0 and S_1. Then for all $A > 0$,*

$$\lim_{T \to +\infty} \sum_k a_k \varphi(x + \Omega_k T) = 0 \tag{19}$$

uniformly with respect to $x \in [-A, A]$.

Proof. Let $\mathcal{F}(x,T) = \sum_k a_k \varphi(x + \Omega_k T)$ and $\varepsilon > 0$. With a Taylor expansion of φ at order n, we have

$$\mathcal{F}(x,T) = \sum_{p=0}^{n} \frac{x^p}{p!} \sum_k a_k \varphi^{(p)}(\Omega_k T) + \frac{x^{n+1}}{(n+1)!} \sum_k a_k \varphi^{(n+1)}(\xi_k) \quad \text{where } \xi_k \in \mathbb{R}\ . \tag{20}$$

We have from lemma 1

$$\left| \frac{x^{n+1}}{(n+1)!} \sum_k a_k \varphi^{(n+1)}(\xi_k) \right| \le \frac{A^{n+1}}{(n+1)!} S_0 \tag{21}$$

and this expression can be made arbitrarily small for sufficiently large values of n. On the other hand, with the notations of lemma 1

$$\left| \sum_k a_k \varphi^{(p)}(\Omega_k T) \right| = \frac{1}{T} \left| \sum_k \frac{a_k}{\Omega_k} (\Omega_k T) \varphi^{(p)}(\Omega_k T) \right| \le \frac{M_p}{T} S_1\ . \tag{22}$$

For any $\varepsilon > 0$, there exists thus $n_0 \in \mathbb{N}$ such that for all $n > n_0$, and all $x \in [-A, A]$,

$$|\mathcal{F}(x,T)| = \frac{S_1}{T} \sum_{p=0}^{n} \frac{A^p}{p!} M_p\ +\ \varepsilon \tag{23}$$

and for T sufficiently large, the sum will be arbitrarily small, which ends the demonstration.

Corollary. 1 *With the hypothesis of lemma 2, we have*

$$\lim_{T \to +\infty} F(x,T) = \varphi(x)\varphi'(x) \tag{24}$$

uniformly for $x \in [-A, +A]$. The function $F(x,T)$ can thus be continuously extended in a function $F^*(x,T) : [-A, A] \times]0, +\infty] \to \mathbb{R}$.

We have also for the derivative

$$\begin{aligned}\frac{\partial F(x,T)}{\partial x} &= \varphi(x)\varphi''(x) + \varphi'^2(x) \\ &+ \sum_k \Re(a_k)\left\{2\varphi'(x)\varphi'(x+\Omega_k T) + \varphi(x)\varphi''(x+\Omega_k T) + \varphi''(x)\varphi(x+\Omega_k T)\right\} \\ &+ \sum_{k,l} \Re(a_k \bar{a}_l)\left\{\varphi(x+\Omega_k T)\varphi''(x+\Omega_l T) + \varphi'(x+\Omega_k T)\varphi'(x+\Omega_l T)\right\} \ .\end{aligned} \tag{25}$$

With the hypothesis of lemma 2, we will have

$$\lim_{T\to+\infty} \frac{\partial F(x,T)}{\partial x} = \varphi(x)\varphi''(x) + \varphi'^2(x) \tag{26}$$

uniformly for $x \in [-A,+A]$. The extension $F^*(x,T)$ thus has a continuous first derivative on $[-A,A]\times]0,+\infty]$. From Lemma 1 and (26), we have $\partial F^*/\partial x\,(0,+\infty) = \varphi''(0) < 0$, we can apply the implicit function theorem (Schwartz, 1992, p.176) to $F^*(x,T)$ at the point $(0,+\infty)$. Thus, there exists a neighborhood U of $+\infty$, and a unique continuous map $\tilde{x}(T) = x$ such that

$$\lim_{T\to+\infty} \tilde{x}(T) = 0; \qquad F(\tilde{x}(T),T) = 0 \quad \text{for all } T \in U \ . \tag{27}$$

Once the existence of $\tilde{x}(T)$ verifying (27) is known, we can obtain a generalized equivalent for $\tilde{x}(T)$ when $T \to +\infty$.

Lemma. 3 *Let $\varphi(x)$ be a function on $\mathbb{R}$, and $n \in \mathbb{N}, n > 0$, and assume that for all $0 \le p \le n$ there exists $M_p > 0$ such that $|x^p\varphi(x)| \le M_p$ for all $x \in \mathbb{R}$. Then, for all $A > 0$, and all $0 \le p \le n$, there exists $N_p > 0$ such that*

$$|X^p\varphi(x+X)| \le N_p \qquad \forall (x,X) \in [-A,+A]\times\mathbb{R} \ . \tag{28}$$

Proof. We have $X^p\varphi(x+X) = (X+x)^p\varphi(x+X) - \sum_{k=0}^{p-1} C_p^k X^k x^{p-k}\varphi(x+X)$ and the proof is obtained by recurrence on p.

Lemma. 4 *Let $\varphi(x)$ be a C^∞ function on $\mathbb{R}$, and assume that*

$$\varphi(x) = \frac{g_0(x)}{x^n} + o\left(\frac{1}{x^n}\right), \qquad \varphi'(x) = \frac{g_1(x)}{x^n} + o\left(\frac{1}{x^n}\right), \tag{29}$$

where $g_0(x)$ and $g_1(x)$ are bounded on $\mathbb{R}$, and that the series $\sum_k \left|\frac{a_k}{\Omega_k^n}\right|$ is convergent. Then for $T \to +\infty$,

$$\sum_k a_k\varphi(x(T)+\Omega_k T) = \sum_k \frac{a_k}{\Omega_k^n T^n} g_0(\Omega_k T) + o\left(\frac{1}{T^n}\right) \ . \tag{30}$$

Proof. Let

$$\mathcal{F}(T) = T^n\left(\sum_k a_k\varphi(x(T)+\Omega_k T) - \sum_k \frac{a_k}{\Omega_k^n T^n} g_0(\Omega_k T)\right) \ . \tag{31}$$

Thus

$$\mathcal{F}(T) = \sum_k \frac{a_k}{\Omega_k^n} \mathcal{F}_k(T) \tag{32}$$

with $\mathcal{F}_k(T) = (\Omega_k T)^n \varphi(x(T) + \Omega_k T) - g_0(\Omega_k T)$. From lemma 3, $|\mathcal{F}_k(T)|$ is bounded, and the series (32) is uniformly convergent with respect to T. We thus have

$$\lim_{T\to+\infty} \mathcal{F}(T) = \sum_k \frac{a_k}{\Omega_k^n} \lim_{T\to+\infty} \mathcal{F}_k(T) \tag{33}$$

But $\varphi(x(T) + \Omega_k T) - \varphi(\Omega_k T) = x(T)\varphi'(\xi_k(T))$ with $|\xi_k(T) - \Omega_k T| \leq |x(T)|$. Thus, as $x^n \varphi'(x)$ is bounded on $\mathbb{R}$, we have for all k

$$\begin{aligned} &\lim_{T\to+\infty} \mathcal{F}_k(T) = \\ &\lim_{T\to+\infty} x(T) \frac{(\Omega_k T)^n}{\xi_k^n(T)} \xi_k^n(T) \varphi'(\xi_k(T)) + (\Omega_k T)^n \varphi(\Omega_k T) - g_0(\Omega_k T) = 0 \ , \end{aligned} \tag{34}$$

which ends the proof of the lemma. We can now complete the proof of theorem 1. Assuming the hypothesis of theorem 1, we can apply this lemma to φ and φ'. We have thus

$$\begin{aligned} \sum_k a_k \varphi(x(T) + \Omega_k T) &= \sum_k \frac{a_k}{\Omega_k^n T^n} g_0(\Omega_k T) + o\left(\frac{1}{T^n}\right) \\ \sum_k a_k \varphi'(x(T) + \Omega_k T) &= \sum_k \frac{a_k}{\Omega_k^n T^n} g_1(\Omega_k T) + o\left(\frac{1}{T^n}\right) \ . \end{aligned} \tag{35}$$

We have also $\varphi(x) = 1 + o(x)$, and $\varphi'(x) = \varphi''(0)x + o(x)$, and $\lim_{T\to+\infty} x(T) = 0$. We can thus make the expansion of the expressions involved in Eq.18 and obtain, by an expansion at first order in x and order n in $1/T$

$$\varphi''(0)x(T) + o(x(T)) + \sum_k \frac{\Re(a_k)}{\Omega_k^n T^n} g_1(\Omega_k T) + o\left(\frac{1}{T^n}\right) = 0 \ , \tag{36}$$

from which the proof of the theorem ends easily. Indeed,

$$T^n x(T) = \frac{-1}{\varphi''(0) + \dfrac{o(x(T))}{x(T)}} \left(\sum_k \frac{\Re(a_k)}{\Omega_k^n} g_1(\Omega_k T) + o(1) \right) , \tag{37}$$

As $\lim_{T\to+\infty} x(T) = 0$, and $\varphi''(0) \neq 0$, then $T^n x(T)$ is bounded and thus $o(x(T)) = o(1/T^n)$ from which

$$x(T) = -\sum_k \frac{\Re(a_k)}{\varphi''(0)\Omega_k^n T^n} g_1(\Omega_k T) + o\left(\frac{1}{T^n}\right) \ . \tag{38}$$

This end the proof of theorem 1. We can then prove the following result

Theorem. 2 *With the hypothesis of theorem 1, for $T \to +\infty$*

$$\nu_1 - \nu_1^T = \frac{-1}{T\varphi''(0)} \sum_k \Re(a_k)\varphi'(\Omega_k T) + O(1/T^{2n+1}) \tag{39}$$

This improvement requires the following lemma :

Lemma. 5 *Let χ be a weight function, $\varphi = \varphi_\chi$ its transform, and assume that*

$$\varphi(x) = \frac{g_0(x)}{x^n} + o\left(\frac{1}{x^n}\right), \qquad \varphi'(x) = \frac{g_1(x)}{x^n} + o\left(\frac{1}{x^n}\right), \quad \varphi''(x) = \frac{g_2(x)}{x^n} + o\left(\frac{1}{x^n}\right), \tag{40}$$

where $g_0(x), g_1(x), g_2(x)$ are bounded on $\mathbb{R}$, and that the series $\sum_k \left|\frac{a_k}{\Omega_k^p}\right|$ is convergent for $p = 0, n$. Then for $T \to +\infty$,

$$\begin{aligned} \sum_k a_k \varphi(x(T) + \Omega_k T) &= \sum_k a_k \varphi(\Omega_k T) + O(1/T^{2n}) \\ \sum_k a_k \varphi'(x(T) + \Omega_k T) &= \sum_k a_k \varphi'(\Omega_k T) + O(1/T^{2n}) \end{aligned} \tag{41}$$

Proof. We will make the proof of the first relation (for $\varphi(x)$); the argument for $\varphi'(x)$ is the same. Let

$$\varphi(x(T) + \Omega_k T) = \varphi(\Omega_k T) + x(T)\varphi'(\Omega_k T) + \frac{x(T)^2}{2}\varphi''(\zeta_k) \tag{42}$$

where $\zeta_k \in [\Omega_k T, \Omega_k T + x(T)]$, and

$$\mathcal{F}(T) = T^{2n}\left(\sum_k a_k \left[\varphi(x(T) + \Omega_k T) - \varphi(\Omega_k T)\right]\right) \tag{43}$$

that is,

$$\mathcal{F}(T) = T^{2n}\sum_k a_k \left[x(T)\varphi'(\Omega_k T) + \frac{x(T)^2}{2}\varphi''(\zeta_k)\right] = \sum_k \mathcal{F}_k(T) \tag{44}$$

From theorem 1, $|T^n x(T)|$ is strictly bounded by a constant N. Moreover, from the hypothesis of the lemma, $x^n\varphi'(x)$ is also bounded by a constant N', and thus $|\Omega_k^n T^n \varphi'(\Omega_k T)| < N'$, and

$$\left|a_k T^{2n} x(T)\varphi'(\Omega_k T)\right| < NN'\left|\frac{a_k}{\Omega_k^n}\right| \tag{45}$$

Finally, $|\varphi''(x)| < 1$ (lemma 1), and as $\left|T^{2n}x(T)^2\right| < N^2$

$$\left|T^{2n}\, a_k \frac{x(T)^2}{2}\varphi''(\zeta_k)\right| < \frac{N^2}{2}\,|a_k|\ . \tag{46}$$

In (44) $|\mathcal{F}_k(T)|$ is thus bounded by $u_k = NN'\left|\frac{a_k}{\Omega_k^n}\right| + \frac{N^2}{2}|a_k|$ which is the general term of a convergent series of sum S, and

$$|\mathcal{F}(T)| \le \sum_k |\mathcal{F}_k(T)| \le \sum_k u_k = S \tag{47}$$

which ends the proof of the lemma. The proof of the theorem can now be completed.
Proof of theorem 2 : From theorem 1, we already know that when $T \to +\infty$, the solution $x(T)$ of EQ. (18) tends to zero and from (38),

$$x(T) = O(1/T^n) \tag{48}$$

We have thus also the expansions for $T \to +\infty$

$$\begin{aligned} \varphi(x(T)) &= 1 + O(1/T^{2n}) \\ \varphi'(x(T)) &= \varphi''(0)x(T) + O(1/T^{3n}) = O(1/T^n); \end{aligned} \tag{49}$$

while Eq.(35) gives

$$\begin{aligned} \sum_k a_k \varphi(x(T) + \Omega_k T) &= O(1/T^n) \\ \sum_k a_k \varphi'(x(T) + \Omega_k T) &= O(1/T^n) \ . \end{aligned} \tag{50}$$

Using these expressions, we can now expand all expressions in Eq.18 up to $O(1/T^{2n})$ which gives

$$\varphi''(0)x(T) + \sum_k \Re(a_k)\varphi'(x(T) + \Omega_k T) = O(1/T^{2n}) \tag{51}$$

and with lemma 5

$$x(T) = -\frac{1}{\varphi''(0)} \sum_k \Re(a_k)\varphi'(\Omega_k T) + O(1/T^{2n}) \tag{52}$$

4.1 Amplitudes

Once the estimate of the precision on the frequencies is obtained, the precision on hte amplitudes is easily calculated. Indeed, with the same notations, the amplitude of the first term of $f(t)$ in eq.14 (which exact value is 1), will be

$$a_1^T =< f(t), e^{i\nu_1^T t} >= \varphi(x(T)) + \sum_k a_k \varphi(x(T) + \Omega_k T) \ . \tag{53}$$

Using the above estimates, one then finds that the error on the amplitude is

$$a_1^T - 1 = \sum_k a_k \varphi(\Omega_k T) + O(1/T^{2n}) = O(1/T^n) \ . \tag{54}$$

5 Cosine windows

We can now apply this theorem to specific examples of weight functions. The most simple weight function will be defined on $[-1, 1]$ as $\chi_0(t) = 1$, with the associate transform

$$\varphi_{\chi_0}(x) = \frac{\sin x}{x} \tag{55}$$

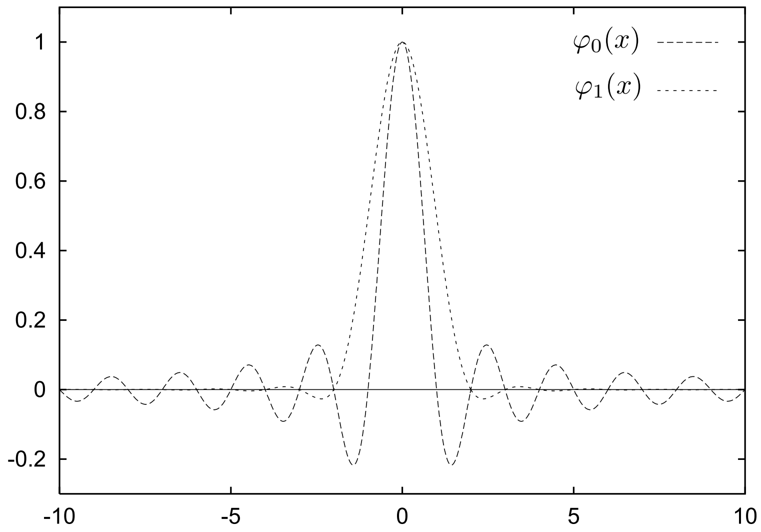

Figure 1: Graph of $\varphi_0(x)$ and $\varphi_1(x)$.

With this window (or absence of window), the decreases of the sidelobes of the transform is slow, (as $1/x$). This is due to the discontinuity at -1 and $+1$ of the window function $\tilde{\chi}_0(x) = 1_{[-1,1]}$, considered as a function on $\mathbb{R}$. In this case, the transform $\varphi_{\tilde{\chi}_0}(x)$ is the usual Fourier transform of $\tilde{\chi}_0(x)$,and it is known that the decrease at infinity of $\varphi_{\tilde{\chi}_0}(x)$ depends on the class of regularity of $\tilde{\chi}_0(t)$. More precisely,

Proposition. 1 *If $f(t)$ is of class C^p on $\mathbb{R}$, absolutely integrable, with all derivatives absolutely integrable, then its Fourier transform $\hat{f}(x)$ satisfies*

$$\hat{f}(x) = \int_{-\infty}^{+\infty} f(t)\, \mathrm{e}^{ixt}\, dt = o(1/x^p) \qquad \textit{when} \qquad |x| \to +\infty \tag{56}$$

We will thus improve the decreasing at infinity of the transform function $\varphi_\chi(x)$ by increasing the class of regularity of the extension to $\mathbb{R}$ of the window function $\chi(t)$. This can be done by using the window function $\chi_1(t) = 1 + \cos \pi\, t$. Indeed, we have then $\chi_1'(t) = -\pi \sin \pi\, t$, $\chi_1''(t) = \pi^2 \cos \pi\, t$ and thus $\chi_1(1) = \chi_1(-1) = \chi_1'(1) = \chi_1'(-1) = 0$, while $\chi_1''(1) = \chi_1''(-1) = \pi^2$. The extension $\tilde{\chi}_1(t)$ is thus C^1 and the decreasing at infinity of the sidelobes of the transform $\varphi_{\chi_1}(x)$ will be much stronger (Fig.1). More generally, we can search for a trigonometric polynomial χ_p such that the extension $\tilde{\chi}_p(t)$ is of class C^p over $\mathbb{R}$. Indeed,

Proposition. 2 *For all $p \in \mathbb{N}$, let $\chi_p(t) = \frac{2^p (p!)^2}{(2p)!}(1 + \cos \pi t)^p$. Then $\chi_p(t)$ is the unique trigonometric polynomial $P(\cos \pi t, \sin \pi t)$ of degree $\leq p$ that is a weight function of class C^{2p-1}. Its associated transform is*

$$\varphi_p(x) = \frac{1}{2} \int_{-1}^{1} e^{ixt}\ \chi_p(t)\ dt = \frac{(-1)^p \pi^{2p} (p!)^2 \sin x}{x(x^2 - \pi^2) \cdots (x^2 - p^2 \pi^2)}\ . \tag{57}$$

Proof. As a weight function is even, P can be expressed uniquely as a polynomial in $\cos \pi t$. Setting $u(t) = \cos \pi t$, the derivatives of $P(u(t))$ are given by the Faa di Bruno formula

$$P(u)^{(k)} = \sum_{r=1}^{k} \sum_{k_1+\cdots+k_r=k} \frac{1}{r!} \frac{k!}{k_1!\cdots k_r!} P^{(r)}(u).u^{(k_1)}\cdots u^{(k_r)} \tag{58}$$

where $k_1, \ldots, k_r \geq 1$. As for $k \geq 0$,

$$\begin{aligned} u^{(2k)}(t) &= \pi^{2k}(-1)^k \cos(\pi t), \\ u^{(2k+1)}(t) &= \pi^{2k+1}(-1)^{k+1} \sin(\pi t); \end{aligned} \tag{59}$$

For $k \geq 0$, we have $u^{(2k+1)}(1) = u^{(2k+1)}(-1) = 0$, and $u^{(2k)}(1) = u^{(2k)}(-1) = (-1)^{k+1}$. The only index k_i for which the contribution in Eq.58 is not zero are thus even, and we obtain

$$P(u)^{(2k+1)}(1) = P(u)^{(2k+1)}(-1) = 0$$

$$P(u)^{(2k)}(1) = P(u)^{(2k)}(-1) = \sum_{r=1}^{k} \sum_{k_1+\cdots+k_r=k} \frac{(-1)^{k+r}}{(r)!} \frac{(2k)!}{(2k_1)!\cdots(2k_r)!} P^{(r)}(-1) \ . \tag{60}$$

To Assume that the weight function is of class C^{2p-1} is equivalent to assume that $P(u)^{(k)}(1) = P(u)^{(k)}(-1) = 0$ for $k = 0, \ldots 2p-1$, that is, from (60), $P^{(k)}(-1) = 0$, for $k = 0, 1, \ldots, p-1$. P is thus a polynomial of the form $P(X) = (1+X)^p\, Q(X)$, where $Q(X)$ is a polynomial, and the proposition follows. The constant is determined such that $1/2 \int_{-1}^{1} \chi_p(t)dt = 1$. We have also easily the asymptotic expansions for $x \to \infty$

$$\varphi_p^{(n)}(x) = \frac{(-1)^p \pi^{2p}(p!)^2 \sin^{(n)} x}{x^{2p+1}} + o\left(\frac{1}{x^{2p+1}}\right) \ ; \tag{61}$$

and the expansion at the origin

$$\varphi_p(x) = 1 + \frac{\varphi_p''(0)}{2} x^2 + o(x^2) \quad \text{with} \quad \varphi_p''(0) = -\frac{2}{\pi^2}\left(\frac{\pi^2}{6} - \sum_{k=1}^{p} \frac{1}{k^2}\right) \tag{62}$$

Thus, if $f(t)$ is a quasi periodic function of the form (14), for which $\sum_k |\frac{a_k}{\Omega_k^m}|$ is convergent for $m = 0, 1$, and $2p+1$; for $T \to +\infty$,

$$\nu_1 - \nu_1^T = \frac{(-1)^{p+1}\pi^{2p}(p!)^2}{\varphi_p''(0) T^{2p+2}} \sum_k \frac{\Re(a_k)}{\Omega_k^{2p+1}} \cos(\Omega_k T) + o\left(\frac{1}{T^{2p+2}}\right) \tag{63}$$

Using theorem 2, we have as well for the cosine windows $\varphi_p(x)$,

$$\nu_1 - \nu_1^T = \frac{-1}{T\varphi_p''(0)} \sum_k \Re(a_k)\varphi_p'(\Omega_k T) + o(1/T^{4p+2}) \tag{64}$$

The computation of the derivative $\varphi_p(x)$ is easy if we write $\varphi_p(x) = C \sin x / D(x)$ where

$$C = (-1)^p \pi^{2p}(p!)^2 \ ; \qquad D(x) = x(x^2 - \pi^2)\cdots(x^2 - p^2\pi^2) \tag{65}$$

Then

$$\varphi_p'(x) = \frac{C}{D(x)}\left[\cos x - \sin x \frac{D'(x)}{D(x)}\right] \tag{66}$$

with

$$\frac{D'(x)}{D(x)} = \frac{1}{x} + \frac{2x}{x^2-\pi^2} + \cdots + \frac{2x}{x^2-p^2\pi^2} \tag{67}$$

5.1 Exponential window

The cosine weight function of order p, $\chi_p(t)$ provides a window function of class C^{2p-1}, and thus improves the convergence of the frequency map algorithm (theorem 1 and 2). Although it will not be always very useful in practice, we can also consider C^∞ windows functions, for which $\chi^{(n)}(-1) = \chi^{(n)}(1) = 0$ for all n, as for example $\chi^*(t) = c\exp(-1/(1-t^2))$, with $c \approx 0.22199690808403971891$. In this case, we have for all values of n, m, $\lim_{x\to+\infty} x^n \varphi_\chi^{(m)}(x) = 0$. Thus, if $\sum_k |\frac{a_k}{\Omega_k^n}|$ are convergent for all m, as for a KAM solution (see below), we will have for all n, $\lim_{T\to+\infty} T^n(\nu_1 - \nu_1^T) = 0$. Let us note that for this exponential window, $\varphi_\chi''(0) \approx -0.035100738376487704994$.

5.2 KAM solutions

If $f(t)$ is a KAM solution, with rotation vector (ν), that fulfills a a diophantine condition (3), it can be expressed as a quasiperiodic series of the form (6),

$$f(t) = \sum_k a_k \mathrm{e}^{i<k,\theta>} \qquad \text{with} \qquad \theta_i = \nu_i t \tag{68}$$

that is analytical with respect to the angles (θ). The series $\sum_k |\frac{a_k}{\Omega_k^p}|$ are then convergent for all p. Indeed, we have then

$$\left|\frac{a_k}{\Omega_k^p}\right| \leq \frac{|a_k|}{\kappa_\varepsilon^p}(1+|k|)^{pm} \ . \tag{69}$$

But due to the analyticity of the series (68) with respect to θ, there exists a small $s > 0$ such that

$$|a_k| \leq ||f||\, \mathrm{e}^{-|k|s} \tag{70}$$

As $|k| = |k_1| + \cdots + |k_n|$, where n is the number of degrees of freedom of the Hamiltonian system,

$$(1+|k|) \leq (1+|k_1|)(1+|k_2|)\dots(1+|k_n|) \tag{71}$$

$$\begin{aligned} \sum_k \left|\frac{a_k}{\Omega_k^p}\right| &\leq \sum_{k_1,\dots,k_n} \frac{||f||}{\kappa_\varepsilon^p}(1+|k_1|)^{pm}\dots(1+|k_n|)^{pm}\mathrm{e}^{-|k|s} \\ &= \frac{||f||}{\kappa_\varepsilon^p} \prod_{i=1,\dots,n} \sum_{k_i\geq 0} (1+|k_i|)^{pm}\mathrm{e}^{-|k_i|s} \ . \end{aligned} \tag{72}$$

These latest series are convergent which ends the proof. In fact, this case will be the most useful, as the solutions we are looking for will usually be the quasiperiodic KAM solutions of an analytical Hamiltonian system. In this case, using the weight χ_p, we can obtain an accuracy for the frequency analysis of order $1/T^{2p+2}$ on these solutions, which gives in particular $1/T^4$ when using the Hanning window (χ_1).

6 Quasiperiodic decomposition

The previous results tell us that with the proposed algorithm, we will recover in a very efficient manner the frequency ν_1 of the leading periodic term of the quasiperiodic decomposition of

$$f(t) = \sum_k A_k \mathrm{e}^{i\nu_k t} \tag{73}$$

A first approximation of the corresponding amplitude A_1 will be given by

$$A_1^{(1)} =< f, e_1 > \qquad \text{where} \qquad e_1 = \mathrm{e}^{i\nu_1 t} \tag{74}$$

we are then left with the remainder

$$f_1 = f- < f, e_1 > e_1 \tag{75}$$

and we can start the process again in order to search for the frequency ν_2 of the next term. A technical complexity appears here, as $e_1 = \mathrm{e}^{i\nu_1 t}$ and $e_2 = \mathrm{e}^{i\nu_2 t}$ are not orthogonal for $<,>_T^\chi$. A classical way to overcome this difficulty is given by Gramm-Schmidt orthogonalization process. Indeed, if $(e_1, \dots, e_n)$ is an independent family of unit vectors, one can construct an orthogonal family $(e'_1, \dots, e'_n)$, such that for all $1 \leq k \leq n$, $Vec(e_1, \dots, e_k) = Vec(e'_1, \dots, e'_k)$, where $Vec(u_1, \dots, u_k)$ denotes the vector space generated by $(u_1, \dots, u_k)$. Indeed,

$$e'_n = \tilde{e}_n / \|\tilde{e}_n\| \quad \text{where} \quad \tilde{e}_n = e_n - \sum_{k=1}^{n-1} < e_n, e'_k > e'k \ , \tag{76}$$

and

$$f_n = f_{n-1} - < f_{n-1}, e'_n > e'_n . \tag{77}$$

As $f_{n-1} \perp Vec(e_1, \dots, e_{n-1}) = Vec(e'_1, \dots, e'_{n-1})$, it is interesting to note, for practical computation that

$$< f_{n-1}, e'_n > = < f_{n-1}, e_n > \ . \tag{78}$$

7 Numerical simulations

The asymptotic convergence of $(\nu_1 - \nu_1^T)$ when $T \to +\infty$ provides a good indication of the possibilities of the method, but in practice, this asymptotic behavior will be also limited by the value of the involved constants, and by numerical accuracy. In the following, the previous asymptotic expressions are tested for a very simple example of a quasiperiodic function. Instead of using the output of a numerical integration, we prefer here to take directly a quasi periodic function with 2 independent frequencies. The tested function is

$$F_1(t) = \frac{1}{1 + 1/2\mathrm{e}^{it} + 1/4\mathrm{e}^{-i\omega t}} \tag{79}$$

with $\omega = 2.02$. This function is chosen because of the slow convergence of its Fourier expansion. The results are displayed in figures 2–6 and Table 1 with a cosine window χ_p of various order $p = 0, 1, 2, 3, 4, 5$, and an exponential window. A second test function $F_2(t)$ is also constructed with the first 50 periodic terms of the frequency decomposition of $F_1(t)$.

7.1 Corrections

Theorems 1 and 2 provide equivalents of the frequency error $(\nu_1 - \nu_1^T)$ when $T \to +\infty$. If a quasiperiodic approximation of $f(t)$ is known, for example by a first frequency analysis, then these estimates can be used as corrections for frequency. It should be noted that when the correction is searched, one does not know the exact values of the perturbing frequencies Ω_k involved in the formulas of theorem 1 and 2, but an approximate value Ω'_k. Under the hypothesis of theorem 1, one has

$$\Omega'_k = \Omega_k + O\left(\frac{1}{T^{n+1}}\right) \tag{80}$$

and the expression (16) is as well valid with Ω'_k instead of Ω_k. In the same way,

$$\varphi''(x) = O\left(\frac{1}{x^n}\right) \quad \text{for} \quad x \longrightarrow +\infty, \tag{81}$$

$$\varphi'(\Omega'_k T) = \varphi'(\Omega_k T) + O\left(\frac{1}{T^{2n}}\right) \tag{82}$$

and the estimation of theorem 2 is also valid with Ω'_k instead of Ω_k. This allows to simplify greatly the use of these corrections as the first estimation is sufficient in general.

7.2 Discussion

We have first analyzed the results of the frequency analysis of $F_1(t)$ for different windows χ_p, and the results of the precision of the determination of the frequency versus the length of the time interval T are given in Figure 2. For each case, the results are fitted with a line and the the results are gathered in Table 1 where a_0 (column 5) is the slope of the straight line least squares fitted to the curves of Fig.2. The same study is then repeated with a correction step provided by theorem 1 and formula (63) using 10 and 50 terms . The results are given in Figures 3–4 and in column a_{10} and a_{50} of Table 1. These values need to be compared with the theoretical value obtained with the full correction of theorem 1, given in column a_∞. The correction obtained with theorem 2 (formula (64)) is then given in column a'_{50}, with a correction computed also with 50 terms.
It should be noted that the correction step improves the determination of the frequency, but only to a certain limit. With $F_1(t)$, it is usually hopeless to expect the approximation in $O(1/T^{2n+1})$ given in theorem 2 (column a'_∞ of Table 1). Indeed, because of the slow decreases of the amplitude of the quasiperiodic expansion of $F_1(t)$, the contribution of the neglected terms will dominate beyond a certain level of precision.

We have then performed the same experience with $F_2(t)$. In this case, the corrections performed with 50 terms can be considered as optimal, as the correction step is now performed with a very precise estimate of the remaining terms. Indeed, the results that are plotted in Figs 6,7, and gathered in columns b_0, b_{50}, b'_{50} of Table 1 are now in much better agreement respectively with the theoretical coefficients a, a_∞, a'_∞.

It is clear from these numerical simulations that even for a perfectly quasiperiodic function, there are some limitation on practical computation of the frequencies, especially when the quasiperiodic expansion is slowly converging. It is nevertheless striking to see that even in the case of a slow convergence, the agreement of a and a_0 is excellent. When the correction is used, there is still a good agreement although not as good, as the effect of the neglected terms will dominate after a certain level of precision, unless, as with $F_2(t)$, the quasiperiodic expansion of the considered function is fully recovered with good accuracy.

p	$-a$	$-a_\infty$	$-a'_\infty$	$-a_0$	$-a_{10}$	$-a_{50}$	$-a'_{50}$	$-b_0$	$-b_{50}$	$-b'_{50}$
0	2	3	3	1.98	2.11	2.97	2.94	1.91	3.15	3.11
1	4	5	7	3.94	4.25	4.90	4.43	3.98	4.81	6.04
2	6	7	11	5.82	6.45	6.35	6.11	5.89	7.01	12.68
3	8	9	15	7.64	7.99	8.01	7.87	8.69	9.49	18.85
4	10	11	19	8.89	9.01	9.03	8.71	11.42	12.48	23.49
5	12	13	23	9.15	9.33	9.33	8.87	13.50	14.47	26.24
$*$				5.46				5.43		

Table 1: Slope of the fitted errors on the frequency. p is the order of the window, a the exponent of the error from eq. (63), a_0 the fitted slope with no correction, a_{10} and a_{50} the correction using 10 or 50 periodic terms and a_∞ the theoretical slope when all terms of equation (63)are used for the correction (providing the series is converging) for the determination of the first frequency of $F_1(t)$ (eq.79). a'_∞ is the same with equation (64). b_0, b_{50}, b'_{50} are the corresponding value for the function $F_2(t)$ obtained as a truncated expansion of $F_1(t)$ with 50 periodic terms.

Overall, it appears that when the quasiperiodic expansion is not fully recovered (up to a certain precision), the correction obtained through equations (63) and (64) does not improve very much the results that can be deduced from the use of a window of higher order (Table 1). Considering that the computation of many terms is time consuming, and that it is not so easy to obtain always the same number of relevant terms for various initial conditions corresponding to different regularity of the solution, I would rather recommend to use different orders for the window of the data. The more the solutions are regular, the higher one can choose the order of the window. Practically, this order is still limited to $p = 3, 5$ for quasi periodic function, and maybe lower for numerical solutions of dynamical systems. When the motion is more chaotic, $p = 1$, or even sometimes $p = 0$ may be preferred. In practice, one would increase the order of the window until the precision seems to decreases and use the highest possible value for p.

7.3 Exponential window

We have also tested the exponential window of section (5.1), and the results are reported for $p = *$ in Table 1, but as it can be seen in Table 1, this was not very successful, compared to the cosine windows. Investigation of different exponential windows should probably be continued, as it is not clear why such windows could not attain the accuracy reached by the cosine windows χ_p.

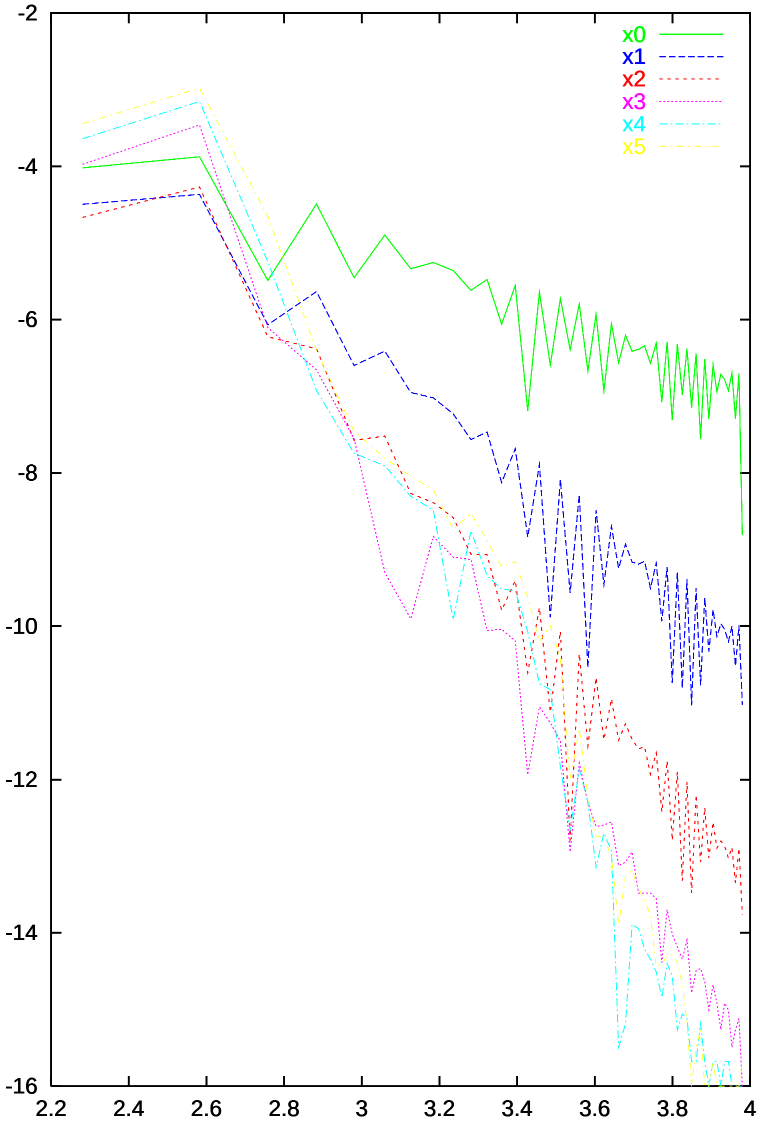

Figure 2: Error on the measured frequency versus duration of the integration for the first frequency of $F_1(t)$. $\log_{10}(err)$ is plotted versus $\log_{10}(T/2\pi)$. x_p is the result for a window of order p .

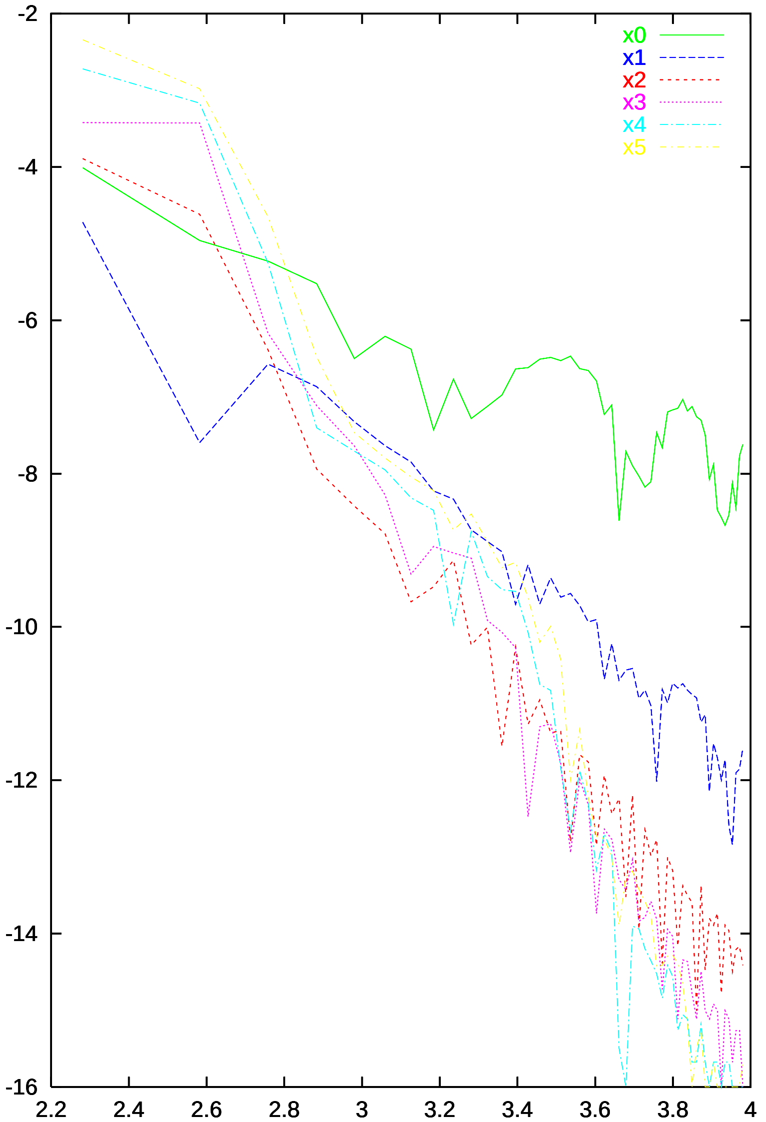

Figure 3: Error on the measured frequency versus duration of the integration for the first frequency of $F_1(t)$. $\log_{10}(err)$ is plotted versus $\log_{10}(T/2\pi)$. x_p is the result for a window of order p with a correction using equation (63) with 10 terms.

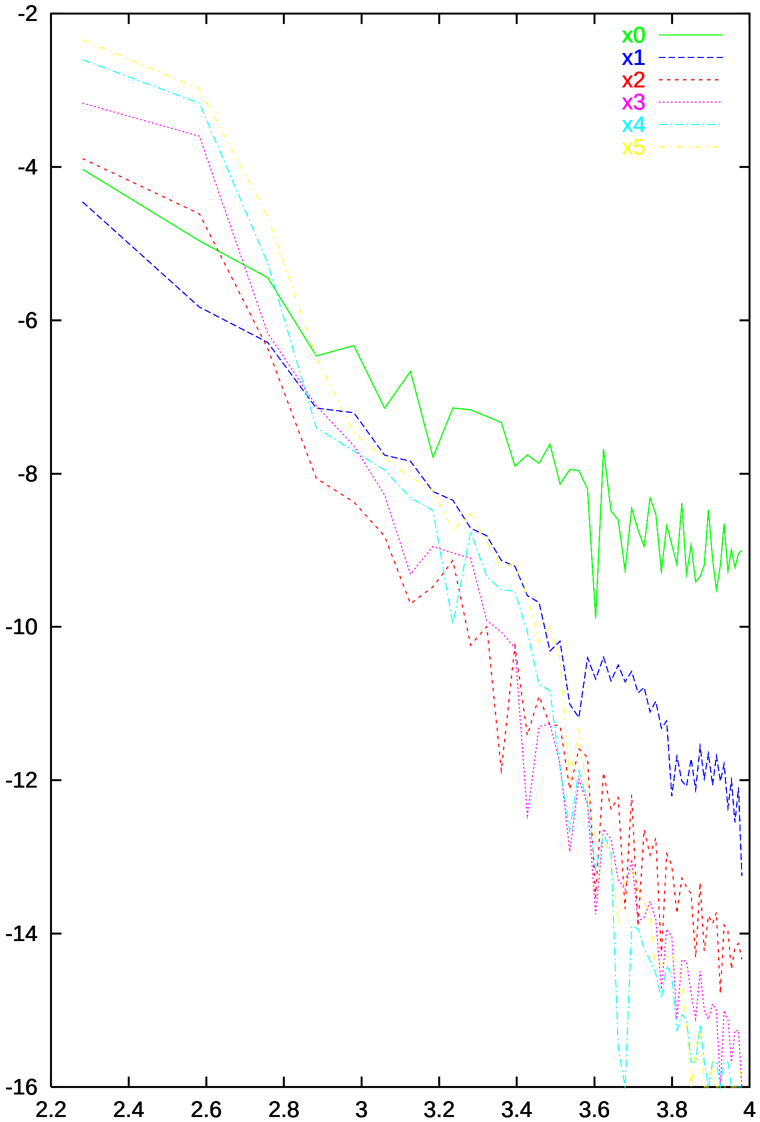

Figure 4: Error on the measured frequency versus duration of the integration for the first frequency of $F_1(t)$. $\log_{10}(err)$ is plotted versus $\log_{10}(T/2\pi)$. x_p is the result for a window of order p with a correction using equation (63) with 50 terms.

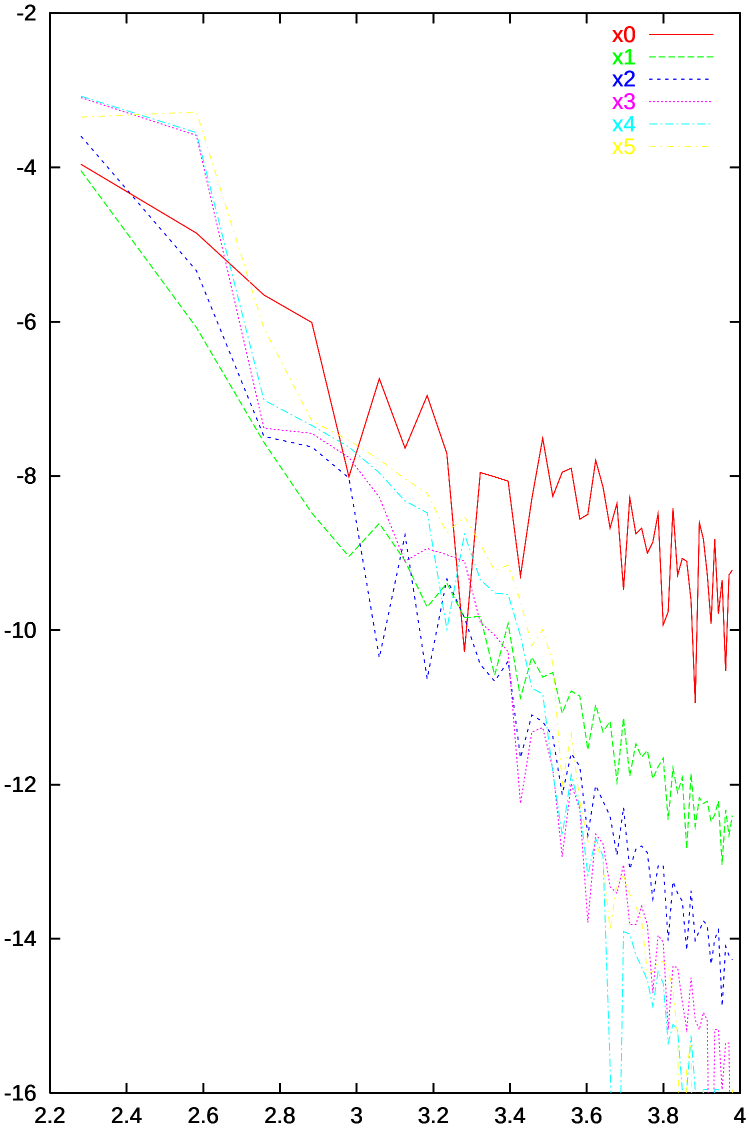

Figure 5: Error on the measured frequency versus duration of the integration for the first frequency of $F_1(t)$. $\log_{10}(err)$ is plotted versus $\log_{10}(T/2\pi)$. x_p is the result for a window of order p with a correction using equation (64) with 50 terms.

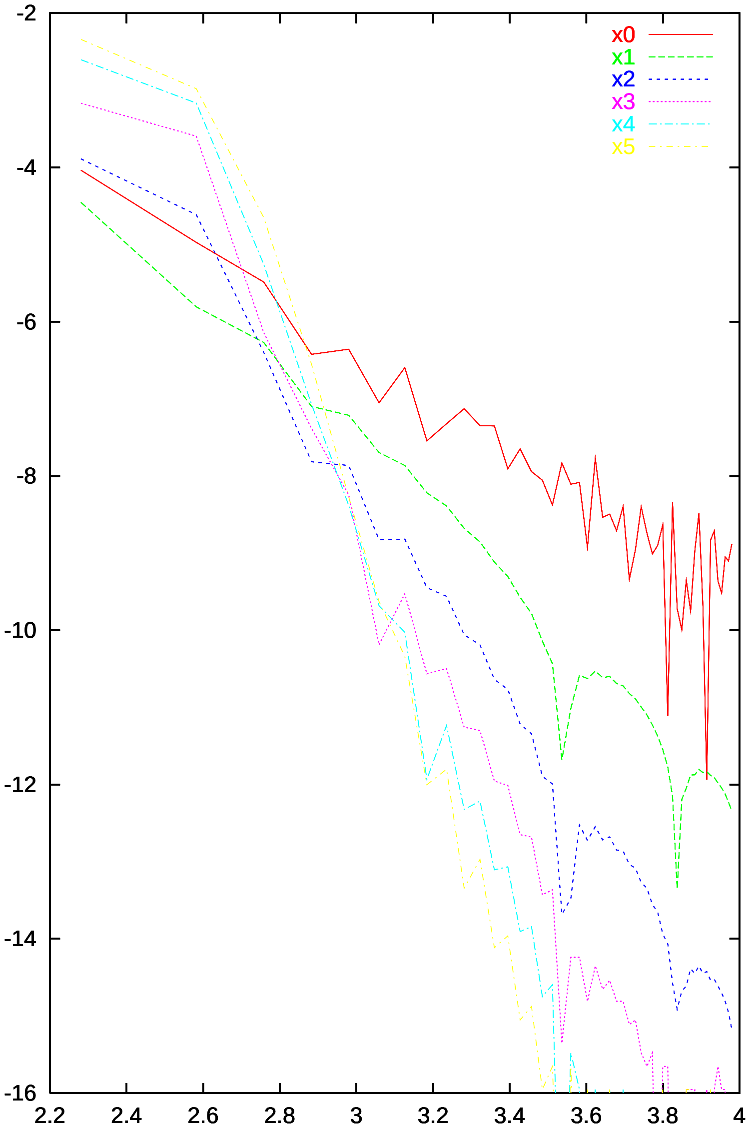

Figure 6: $F_2(t)$. Error on the measured frequency versus duration of the integration for the first frequency of $F_2(t)$. $\log_{10}(err)$ is plotted versus $\log_{10}(T/2\pi)$. x_p is the result for a window of order p with a correction using equation (63) with 50 terms.

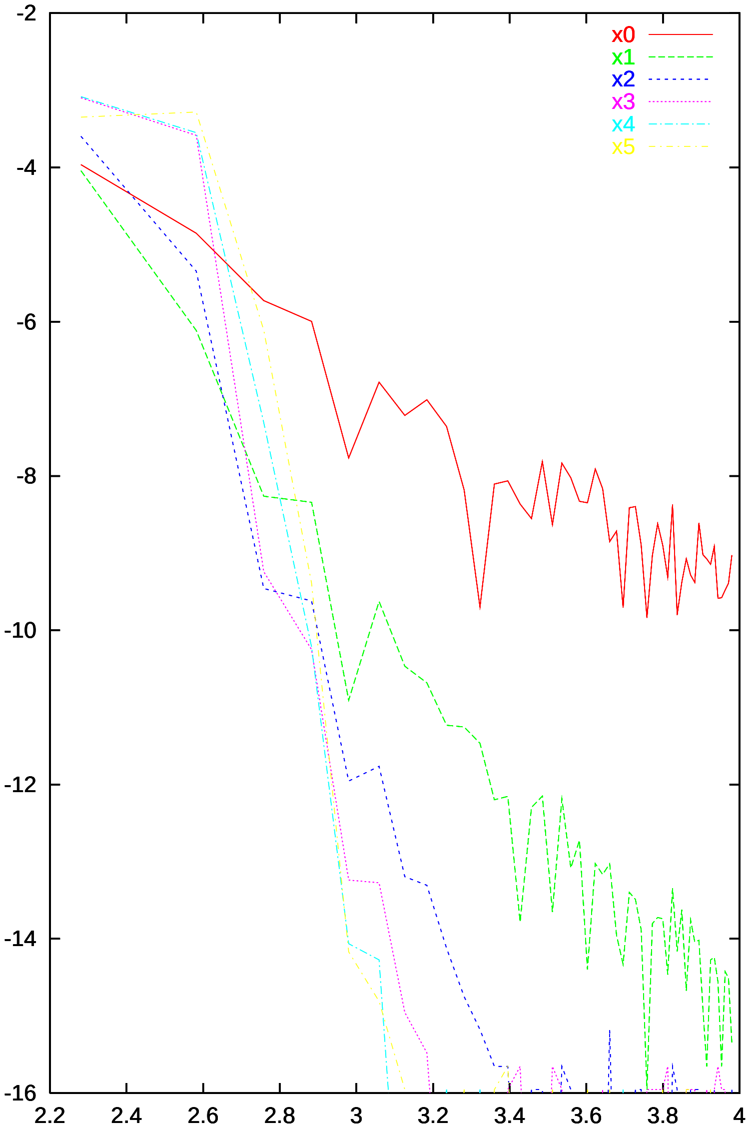

Figure 7: $F_2(t)$. Error on the measured frequency versus duration of the integration. $\log_{10}(err)$ is plotted versus $\log_{10}(T/2\pi)$ for the first frequency of $F_2(t)$. x_p is the result for a window of order p with a correction using equation (64) with 50 terms.

8 Beyond Nyquist frequency

8.1 Nyquist frequency

A typical limitation in spectral analysis is given by the so called Nyquist frequency. Roughly speaking, it will not be possible to determine a frequency ν larger than π/h, where h is the sampling time interval of the observed data. If $|\nu_0| > \pi/h$, the observed frequency will become $\nu = \nu_0 + k2\pi/h$, where $k \in \mathbb{Z}$ such that $|\nu| < \pi/h$. This is actually what can be observed using the NAFF algorithm detailed above.

ν_0/π	ν/π	$(\nu_0 - \nu)/\pi$
0.990	0.990	0.000000000000000000
0.991	0.991	0.000000000000000000
0.992	0.992	0.000000000000000000
0.993	0.993	0.000000000000000000
0.994	0.994	0.000000000000000000
0.995	0.995	0.000000000000000000
0.996	0.996	0.000000000000000000
0.997	0.997	0.000000000000000000
0.998	0.998	0.000000000000000000
0.999	0.999	0.000000000000000000
1.000	−1.000	2.000000000000000000
1.001	−0.999	2.000000000000000000
1.002	−0.998	2.000000000000000000
1.003	−0.997	2.000000000000000000
1.004	−0.996	2.000000000000000000
1.005	−0.995	2.000000000000000000
1.006	−0.994	2.000000000000000000
1.007	−0.993	2.000000000000000000
1.008	−0.992	2.000000000000000000
1.009	−0.991	2.000000000000000000

Table 2: The function $\exp(i\nu_0 t)$ is evaluated for $t = -1000, 1000$, with a stepsize $h = 1$. For $\nu_0/\pi < h$, the recovered frequency (ν) is recovered by NAFF up to the machine precision, but for $\nu_0/\pi > h$, the recovered frequency is here $\nu_0 - 2\pi/h$.

8.2 Multiple timescales problem

The Nyquist aliasing constraint means that to recover a given period, one needs to sample the data with at least two points per period. On the opposite, in order to determine precisely the long periods, one needs that the total interval length T is several time larger than these periods, in order to reach the asymptotic rates of theorems 1 and 2, or to be able to separate properly close frequencies. One thus realizes that if good low frequency determination imposes that T is large, while high frequencies impose that h is small, we will face a problem when two very different time scales are present in the system. This is actually the case

for planetary systems where short periods (of the order of the year) are present, as well as long secular periods, ranging, in the Solar system for example, from 40 000 years to a few millions of years (Laskar, 1990).
The first frequency analysis of the solar system solutions were made uniquely on the output of the secular equations, where only the long periods were present (Laskar, 1988), but if we want now to perform a frequency analysis of the direct output of a numerical integration of Newton's equations, without filtering or averaging, both time scales will be present.
For the Solar system, for example, the determination of the long secular frequencies with a good accuracy will require that T is larger than 20 millions of years, while the sampling h must be smaller than half of the shortest period of the system, that is a few days if we consider the Moon motion, while $h = 5000$ years was enough for the secular equations. The amount of data to handle becomes then considerable as well as the related numerical computations.

8.3 Multiple timescales solution

The solution that can be use to overcome this problem is simply to sample the data with two different sampling intervals that are very close h and $h' = h + \varepsilon$. For a real x, we will denote $[x]$ the integer such that

$$-\frac{1}{2} < x - [x] \leq \frac{1}{2} \; . \tag{83}$$

With this notation, the frequency analysis of $f(t) = \exp(i2\pi\nu_0 t)$ will give a frequency $2\pi\nu$ such that

$$\nu_0 h = \nu h + k \qquad \text{with} \qquad k = [\nu_0 h] \; . \tag{84}$$

The Nyquist condition is then expressed by the fact that $|\nu_0 h| < 1/2$ implies $k = 0$. We assume now that the second sampling time interval $h' = h + \varepsilon$ is such that

$$|\nu_0 \varepsilon| < \frac{1}{2} \; . \tag{85}$$

We have then

$$\begin{aligned} \nu_0 h' = \nu_0 (h + \varepsilon) &= \nu h + \varepsilon \nu_0 + k \\ &= \nu' (h + \varepsilon) + k' \end{aligned} \tag{86}$$

with

$$k' = k + [\nu h + \varepsilon \nu_0] \tag{87}$$

and thus

$$\nu' h' - \nu h = \varepsilon \nu_0 - [\nu h + \varepsilon \nu_0] \; . \tag{88}$$

As $|\nu_0 \varepsilon| < 1/2$,

$$[\nu' h' - \nu h] = -[\nu h + \varepsilon \nu_0] \; , \tag{89}$$

and thus, from (88),

$$\nu_0 = \frac{1}{h' - h} \left(\nu' h' - \nu h - [\nu' h' - \nu h] \right) \; , \tag{90}$$

which allows to revover in all cases the true value of the frequencies. Practically, although this formula can be used, there is an easy way to reduce the numerical errors of these computations. Indeed, it is easy to see that

$$k = \frac{h}{h' - h}((\nu' - \nu)h' - [\nu' h' - \nu h]) \ , \tag{91}$$

which allows to recover ν_0 through (84). The main advantage of this intermediary step is that as k should be an integer, the computed value can be rounded to its nearest integer and

$$\nu_0 = \nu + \frac{[k]}{h} \ . \tag{92}$$

8.4 Numerical examples

8.4.1 Single periodic term

In order to evaluate numerically the efficiency of the method described above, we first used a function $f(t) = \exp(i\nu_0 t)$ with a single periodic term of frequency ν_0. $f(t)$ is evaluated from -1000 to $+1000$, with a stepsize $h = 1$, and the frequency analysis is performed with different values of ν_0, for values of ν_0/π higher than 1000. The value ν_0 is only recovered for $\nu_0/\pi < 1$ (Table 2), but for larger values of ν_0, the use of a second stepsize $h' = 1.001$ and formula (91,92) allows to recover the true frequency for values of ν_0/π as high as 1000 with great accuracy (Table 3).

8.4.2 Sun-Jupiter-Saturn system

As a second, and more realistic example, we have consider a full numerical integration of the Sun-Jupiter-Saturn system over 50 millions of years. The numerical integration is performed with the symplectic integrator $SBAB_3$ that is well adapted to perturbed Hamiltonian systems (Laskar and Robutel, 2001). In order to illustrate the previous section, we have performed the frequency analysis of the variable $z_5 = e_5 \exp(i\varpi_5)$ (Fig.4), where e_5 is the eccentricity of Jupiter, and ϖ_5 its longitude of perihelion, and the analysis of $\sin(i_5/2)\exp(i\Omega_5)$ (Fig.5), where i_5 and Ω_5 are the inclination and longitude of the node with respect to the ecliptic and equinox J2000 reference frame. If one considers the invariance of the angular momentum, this problems has 5 degrees of freedom, that should correspond to 5 fundamental frequencies for a regular KAM solution. These frequencies will be n_5, n_6, the mean mean motion of Jupiter and Saturn, g_5, g_6 related to the precessional motion of the perihelion of Jupiter and Saturn, and s_6 related to the motion of the node of the two orbits (see Laskar, 1990). In the integration, we used an output stepsize of 200 years, while the integration stepsize is 0.1 year. This allows to recover precisely the secular frequencies of the system, but as the short period perturbations are important, many terms appear in the quasiperiodic decomposition that are in fact aliased terms coming from the short period terms (see Table 4,5).
When we use an additional output time $h' = 200.0002$ years, and formula (91,92), we can recover the true value of the aliased frequencies ν_{0i}, even if some of the periods are smaller than 6 years (columns P_i). In Table 4, 5, k is the integer appearing in formula (84), denoting the number of turns that have

ν_0/π	ν/π	ν'/π	ν_f/π
0.500	0.500000	0.500500	0.500000000000
1.000	-1.000000	-0.999000	1.000000000000
1.500	-0.500000	-0.498500	1.500000000000
2.000	-0.000000	0.002000	2.000000000000
2.500	0.500000	0.502500	2.500000000000
3.000	-1.000000	-0.997000	3.000000000000
3.500	-0.500000	-0.496500	3.500000000000
4.000	-0.000000	0.004000	4.000000000000
4.500	0.500000	0.504500	4.500000000000
5.000	-1.000000	-0.995000	5.000000000000
990.000	0.000000	0.990000	990.000000000000
990.500	0.500000	-0.509500	990.500000000000
991.000	-1.000000	-0.009000	991.000000000000
991.500	-0.500000	0.491500	991.500000000000
992.000	-0.000000	0.992000	992.000000000000
992.500	0.500000	-0.507500	992.500000000000
993.000	-1.000000	-0.007000	993.000000000000
993.500	-0.500000	0.493500	993.500000000000
994.000	-0.000000	0.994000	994.000000000000
994.500	0.500000	-0.505500	994.500000000000
995.000	-1.000000	-0.005000	995.000000000000
995.500	-0.500000	0.495500	995.500000000000
996.000	-0.000000	0.996000	996.000000000000
996.500	0.500000	-0.503500	996.500000000000
997.000	-1.000000	-0.003000	997.000000000000
997.500	-0.500000	0.497500	997.500000000000
998.000	-0.000000	0.998000	998.000000000000
998.500	0.500000	-0.501500	998.500000000000
999.000	-1.000000	-0.001000	999.000000000000
999.500	-0.500000	0.499500	999.500000000000
1000.000	-0.000000	-1.000000	1000.000000000000
1000.500	0.500000	-0.499500	-999.500000000000
1001.000	-1.000000	0.001000	-999.000000000000
1001.500	-0.500000	0.501500	-998.500000000000
1002.000	-0.000000	-0.998000	-998.000000000000
1002.500	0.500000	-0.497500	-997.500000000000
1003.000	-1.000000	0.003000	-997.000000000000

Table 3: The function $\exp(i\nu_0 t)$ is evaluated for $t = -1000, 1000$, with a stepsize $h = 1$, and with $h' = 1.001$. The reconstruction formula (91,92) allows to obtain the correct frequency up to $\nu_0/\pi = 1000$.

ν_{0i}	P_i (years)	k	$\|A_i\| \times 10^8$	k_{1i}	k_{2i}	k_{3i}	k_{4i}	k_{5i}
4.027808	321763.1	0	4412046	0	0	1	0	0
28.013748	46263.0	0	1592683	0	0	0	1	0
−21264.867867	−60.9	−3	64449	−1	2	0	0	0
51.999689	24923.2	0	62876	0	0	−1	2	0
1410.142247	919.1	0	38666	−2	5	0	−2	0
22703.023863	57.1	4	13141	−1	3	0	−1	0
−86525.641213	−15.0	−13	10467	−2	3	0	0	0
1386.156306	935.0	0	9940	−2	5	1	−3	0
43995.905478	29.5	7	8056	0	1	0	0	0
−42557.749483	−30.5	−7	6449	−2	4	0	−1	0
−21240.881927	−61.0	−3	4605	−1	2	−1	1	0
−21288.853808	−60.9	−3	4294	−1	2	1	−1	0
−151786.414559	−8.5	−23	3662	−3	4	0	0	0
75.985629	17055.9	0	3493	0	0	−2	3	0
109256.678825	11.9	17	3448	1	0	0	0	0
1434.128187	903.7	0	2485	−2	5	−1	−1	0
−107818.522829	−12.0	−17	2015	−3	5	0	−1	0
−19.958132	−64935.9	0	1929	0	0	2	−1	0
22679.037922	57.1	3	1852	−1	3	1	−2	0
1362.170366	951.4	0	1824	−2	5	2	−4	0
−217047.187912	−6.0	−33	1503	−4	5	0	0	0
239778.225515	5.4	37	1473	3	−2	0	0	0
−86501.655273	−15.0	−13	1217	−2	3	−1	1	0
−80.092473	−16181.3	0	1175	0	0	0	−1	2
−42581.735423	−30.4	−7	1173	−2	4	1	−2	0
−86549.627153	−15.0	−13	1149	−2	3	1	−1	0
1458.114127	888.8	0	1103	−2	5	−2	0	0
87963.797209	14.7	14	1073	0	2	0	−1	0
−22646.996366	−57.2	−3	1060	1	−3	0	3	0
21320.895355	60.8	3	1031	1	−2	0	2	0
87987.783148	14.7	14	932	0	2	−1	0	0
−173079.296175	−7.5	−27	909	−4	6	0	−1	0
305038.998861	4.2	47	820	4	−3	0	0	0
−63850.631098	−20.3	−10	805	−3	6	0	−2	0
2792.270745	464.1	0	793	−4	10	0	−5	0
−19882.739378	−65.2	−3	761	−3	7	0	−3	0
65288.787089	19.9	10	723	1	−1	0	1	0
66670.915597	19.4	10	711	−1	4	0	−2	0
−56.106533	−23098.9	0	679	0	0	−1	0	2
−282307.961256	−4.6	−44	655	−5	6	0	0	0
−151762.428619	−8.5	−23	599	−3	4	−1	1	0
−151810.400498	−8.5	−23	573	−3	4	1	−1	0
174517.452169	7.4	27	545	2	−1	0	0	0
−43939.877972	−29.5	−7	511	0	−1	0	2	0
−65256.745538	−19.9	−10	502	−1	1	1	0	0
−107842.508766	−12.0	−17	454	−3	5	1	−2	0
−238340.069522	−5.4	−37	450	−5	7	0	−1	0
2768.284805	468.2	0	430	−4	10	1	−6	0
370299.772209	3.5	57	428	5	−4	0	0	0
−21312.839748	−60.8	−3	427	−1	2	2	−2	0

Table 4: Frequency analysis of $z_5 = e_5 \exp(i\varpi_5)$ in the Sun-Jupiter-Saturn system. The integration of the complete Newton equations is performed over 50 myr with two output stepsizes $h = 200$ yr and $h' = 200.0002$ yr. ν_{0i} are the reconstructed frequencies using formula (91,92) and the two step sizes h and h'. P_i is the period of the terms, while A_i their amplitude. The different frequencies are identified as integer combination s of the fundamental frequencies $\nu_{0i} = k_{1i}n_5 + k_{2i}n_6 + k_{3i}g_5 + k_{4i}g_6 + k_{5i}s_6$

ν_{0i}	P_i (years)	k	$\|A_i\| \times 10^8$	k_{1i}	k_{2i}	k_{3i}	k_{4i}	k_{5i}
−26.039362	−49770.8	0	315418	0	0	0	0	1
0.000000		0	59173	0	0	0	0	0
82.066859	15792.0	0	1457	0	0	0	2	−1
1464.195357	885.1	0	873	−2	5	0	−1	−1
58.080919	22313.7	0	820	0	0	1	1	−1
−50.025302	−25906.9	0	666	0	0	1	−1	1
34.094979	38011.5	0	623	0	0	2	0	−1
−2.053422	−631141.6	0	285	0	0	−1	1	1
22757.076973	56.9	4	228	−1	3	0	0	−1
106.052799	12220.3	0	197	0	0	−1	3	−1
1440.209417	899.9	0	168	−2	5	1	−2	−1
65234.733984	19.9	10	93	1	−1	0	0	1
88017.850319	14.7	14	92	0	2	0	0	−1
−65286.812708	−19.9	−10	82	−1	1	0	0	1
−42503.696373	−30.5	−7	74	−2	4	0	0	−1
21266.842254	60.9	3	71	1	−2	0	1	1
130495.507329	9.9	20	61	2	−2	0	0	1
−21318.920978	−60.8	−3	58	−1	2	0	−1	1
153278.623665	8.5	24	39	1	1	0	0	−1
−1408.167857	−920.3	0	38	2	−5	0	3	1
218539.397009	5.9	34	37	2	0	0	0	−1
21242.856314	61.0	3	34	1	−2	1	0	1
−21234.800697	−61.0	−3	32	−1	2	1	0	−1
−74.011242	−17510.9	0	30	0	0	2	−2	1
−43993.931092	−29.5	−7	28	0	−1	0	1	1
43941.852367	29.5	7	28	0	1	0	−1	1
1512.167238	857.0	0	27	−2	5	−2	1	−1
1416.223477	915.1	0	26	−2	5	2	−3	−1
195756.280683	6.6	30	26	3	−3	0	0	1
−130547.586054	−9.9	−20	25	−2	2	0	0	1
66724.968703	19.4	10	25	−1	4	0	−1	−1
86527.615599	15.0	13	24	2	−3	0	1	1
22781.062913	56.9	4	23	−1	3	−1	1	−1
1356.089136	955.7	0	19	−2	5	0	−3	1
21.932518	59090.3	0	19	0	0	−2	2	1
283800.170356	4.6	44	19	3	−1	0	0	−1
44025.972649	29.4	7	17	0	1	1	0	−1
−107764.469717	−12.0	−17	17	−3	5	0	0	−1
130.038740	9966.3	0	17	0	0	−2	4	−1
2846.323859	455.3	0	16	−4	10	0	−4	−1
22733.091033	57.0	4	15	−1	3	1	−1	−1
131985.742049	9.8	20	15	0	3	0	−1	−1
−63796.577987	−20.3	−10	14	−3	6	0	−1	−1
−19828.686253	−65.4	−3	14	−3	7	0	−2	−1
−22701.049474	−57.1	−4	13	1	−3	0	2	1
−21210.814756	−61.1	−3	13	−1	2	0	1	−1
−86579.694320	−15.0	−13	12	−2	3	0	−1	1
−1384.181921	−936.3	0	12	2	−5	−1	4	1
261017.054022	5.0	40	12	4	−4	0	0	1
44049.958588	29.4	7	11	0	1	0	1	−1

Table 5: Same as Table 4 for $\sin(i_5/2)\exp(i\Omega_5)$, where i_5 and Ω_5 are the inclination and longitude of the node with respect to the ecliptic and equinox J2000 reference frame. The constant term is due to the invariance of the angular momentum. It would not be present in the reference frame of the invariant plane, orthogonal to the angular momentum of the system.

	(arcsec/years)
n_5	109256.6788245339
n_6	43995.9054783976
g_5	4.0278083375
g_6	28.0137484932
s_6	-26.0393621745

Table 6: Fundamental frequencies of the Sun-Jupiter-Saturn system, obtained by frequency analysis over 50 myr.

been "lost" by the large stepsize. All the determined frequencies ν_{0i} can then be identified as integer combinations

$$\nu_{0i} = k_{1i} n_5 + k_{2i} n_6 + k_{3i} g_5 + k_{4i} g_6 + k_{5i} s_6 \tag{93}$$

of the fundamental frequencies n_5, n_6, g_5, g_6, s_6 given in Table 5. The full solution can then be compared to the quasiperiodic solution obtained by iteration of (Bretagnon and Simon, 1990).
The presence of a constant term in Table 5 is due to the invariance of the angular momentum. It would not be present in the reference frame of the invariant plane, orthogonal to the angular momentum of the system (see Malige *et al.*, 2002).
The existence of short periods is thus not an obstacle, and the aliasing problem can be overcome, as in practice, using two output time steps is not a big constraint. It should not be costly in term of CPU time, as the two output are generated during the same integration. The large advantage of this procedure versus the numerical averaging that was usually performed online (as in Nobili *et al.*, 1989), is that no information is lost, and the whole solution can be recovered.

Acknowledgements The author is very obliged to A. Chenciner, F. Joutel, L. Niederman and D. Sauzin for very useful discussions at several stages of this work. The help of F. Joutel and P. Robutel for the numerical comparisons is deeply appreciated.

References

[1] Arnold, V.I., Kozlov, V.V., Neishtadt, A.I.: 1988, Mathematical aspects of classical and celestial mechanics, *Dyn. Systems III*, V.I. Arnold, ed., Springer, New York.

[2] Arnold, V.I.: 1989, Mathematical Methods of Classical Mechanics, Springer, New York.

[3] Bretagnon, P., Simon, J.-L.: 1990, Théorie générale du couple Jupiter-Saturne par une méthode itérative, *Astron. Astrophys.*, **239**,387–398

[4] Chandre, C., Laskar, J., Benfatto, G., Jauslin, H.R.: 2001, Determination of the breakup of invariant tori in three frequency Hamiltonian systems *Physica D*, **154**, p. 159–170

[5] Comunian, M., Pisent, A., Bazzani, A., Turchetti, G., Rambaldi, S.:2001, Frequency map analysis of a three-dimensional particle in the core model of a high intensity linac, *Phys. Rev. ST Accel. Beams* **4**, 124201 (2001)

[6] Dumas, S., Laskar, J. : 1993, Global Dynamics and Long-Time Stability in Hamiltonian Systems via Numerical Frequency Analysis, *Phys. Rev. Lett.*, **70**, (2975-2979)

[7] Laskar, J. : 1990, The chaotic motion of the solar system. A numerical estimate of the size of the chaotic zones, *Icarus*, **88**, (266-291)

[8] Laskar, J. : 1993, Frequency analysis for multi-dimensional systems. Global dynamics and diffusion, *Physica D*, **67**, (257-281)

[9] Laskar, J. : 1999, Introduction to frequency map analysis, *in proc. of NATO ASI Hamiltonian Systems with Three or More Degrees of Freedom, C. Simò ed, Kluwer*, (134-150)

[10] Laskar, J.: 2000, Application of frequency map analysis in galactic dynamics, *in proc. The Chaotic Universe, Rome, Pescara, 1–5 fev 1999*, V. Gurdzadyan and R. Ruffini, eds., World Scientific, p. 115–126

[11] Laskar, J., Froeschlé, C., Celletti, A. : 1992, The measure of chaos by the numerical analysis of the fundamental frequencies. Application to the standard mapping, *Physica D*, **56**, (253-269)

[12] Laskar, J., Robutel, P. : 1993, The chaotic obliquity of the planets, *Nature*, **361**, (608-612)

[13] Laskar, J., Robutel, P. : 2001, High order symplectic integrators for perturbed Hamiltonian systems, *Celest. Mech.*, **80**, 39–62

[14] Laskar, J., Robin, D. : 1996, Application of frequency map analysis to the ALS, *Particle Accelerator*, **54**, (183-192)

[15] Malige, F., Robutel, P., Laskar, J.: 2002, Partial Reduction in the N-Body Planetary Problem using the Angular Momentum Integral, *Celest. Mech.*, **84**, 283-316

[16] Merritt, D., Valluri, M.: 1999, Resonant Orbits in Triaxial Galaxies *Astron. J.*,**118**, 1177–1189

[17] Nesvorný, D., Ferraz-Mello, S. : 1997, Chaotic diffusion in the 2/1 asteroidal resonance: an application of the frequency map analysis, *Astron. Astrophys.*, **320**, (672)

[18] Nobili, A.M., Milani, A., Carpino, M. : 1989, Fundamental frequencies and small divisors in the orbits of the outer planets, *Astron. Astrophys.*, **210**, (313–336)

[19] Papaphilippou, Y., Laskar, J. : 1996, Frequency map analysis and global dynamics in a two degrees of freedom galactic potential, *Astron. Astrophys.*, **307**, (427-449)

[20] Papaphilippou, Y., Laskar, J. : 1998, Global dynamics of triaxial galactic models through frequency map analysis, *Astron. Astrophys.*, **329**, (451-481)

[21] Papahilippou, Y. Zimmermann, F. :2002, Estimates of diffusion due to long-range beam-beam collisions *Phys. Rev. ST Accel. Beams* **5**, 074001 (2002)

[22] Robin, D., Steir, C., Laskar, J., Nadolski, L.: 2000, Global dynamics of the ALS revealed through experimental Frequency Map Analysis, *Phys. Rev. Let.*, **85**, pp. 558-561

[23] Robutel, P., Laskar, J.: 2001, Frequency Map and Global Dynamics in the Solar System I: Short period dynamics of massless particles, *Icarus*, **152**, 4–28

[24] Schwartz, L: 1992, Analyse, t.II. Calcul différentiel et équations différentielles, *Hermann, Paris*

[25] Steier, C., Robin, D., Nadolski, L., Decking, W., Wu, Y., Laskar, J.: 2002, Measuring and optimizing the momentum aperture in a particle accelerator, *Phys. Rev. E*, **65**, (056506)

[26] Valluri, M., Merritt, D.: 1998 Regular and Chaotic Dynamics of Triaxial Stellar Systems *Astrophys. J.*,**506**, 686–711

[27] Von Milczewski, J., Farrelly, D. Uzer, T.: 1997, Frequency Analysis of 3D Electronic 1/r Dynamics: Tuning between Order and Chaos *Phys. Rev. Let.*, **78**, 1436–1439

[28] Wachlin, F. C.; Ferraz-Mello, S.: 1998, Frequency map analysis of the orbital structure in elliptical galaxies *M.N.R.A.S.* **298**, 1, 22–32